Predator detection through active photolocation in a diurnal fish

Matteo Santon[1], Pierre-Paul Bitton[1,3], Jasha Dehm[1,2], Roland Fritsch[1], Ulrike K. Harant[1], Nils Anthes[1], Nico K. Michiels[1]*.

[1]Animal Evolutionary Ecology, Institute of Evolution and Ecology, Department of Biology, Faculty of Science, University of Tübingen, Auf der Morgenstelle 28, 72076 Tübingen, Germany.

[2] School of Marine Studies, Faculty of Science, Technology & Environment, University of the South Pacific, Laucala Bay Rd., Suva, Fiji.

[3] Department of Psychology, Memorial University of Newfoundland, 232 Elizabeth Avenue, St. John's, NL A1B 3X9, Canada

***Correspondence to:** nico.michiels@uni-tuebingen.de

Abstract: A recent study showed that triplefins, small cryptobenthic fish, actively reflect downwelling light sideways using their irides. Here, we investigate whether they do this to break the camouflage of cryptic predators by inducing eyeshine, revealing their presence. We attached mini-shades to triplefins to block light redirection and monitored the distance they kept to a cryptic sit-and-wait predator, a scorpionfish with retroreflective eyes. Shaded triplefins stayed significantly closer than two control treatments in replicate laboratory and field experiments. When confronted with a stone as a control, the treatments did not differ in their behaviour. Visual modelling confirmed that the light redirected by a triplefin is sufficient to increase the brightness of a nearby scorpionfish's pupil to a degree that can be visually detected by that triplefin. We conclude that small fish detect nearby cryptic predators better when allowed to redirect light from their irides. This new form of active sensing, called diurnal active photolocation, has wide implications for fish eye evolution.

Nocturnal and deep-sea fish with a chemiluminescent search light are currently the only known vertebrates to use light for active sensing[1,2]. However, recent findings suggest small fish may benefit from a previously undescribed, diurnal form of active photolocation that rests on several unique mechanisms allowing fish to redirect downwelling sunlight. We focus on a behaviour called "ocular spark"[3], where the protruding lens focuses downwelling light onto the lower iris. The resultant ocular spark allows fish to redirect sunlight outside the range dictated by Snell's window[4], which constrains downwelling sunrays to a 96° cone pointing down from the surface. Previous work in the triplefin *Tripterygion delaisi* showed that ocular sparks are under behavioural control and increase in frequency in a prey detection context (Fig. 1a-b)[3]. The authors hypothesized that ocular sparks produce sufficient light to improve visual detection of cryptic target organisms. Indeed, the close vicinity between an ocular spark and the pupil is analogous to that of the subocular light organ in some chemiluminescent fishes[2,5-9]. This configuration has been interpreted as an adaptation to induce and detect retroreflective eyeshine in other organisms[1,3,10].

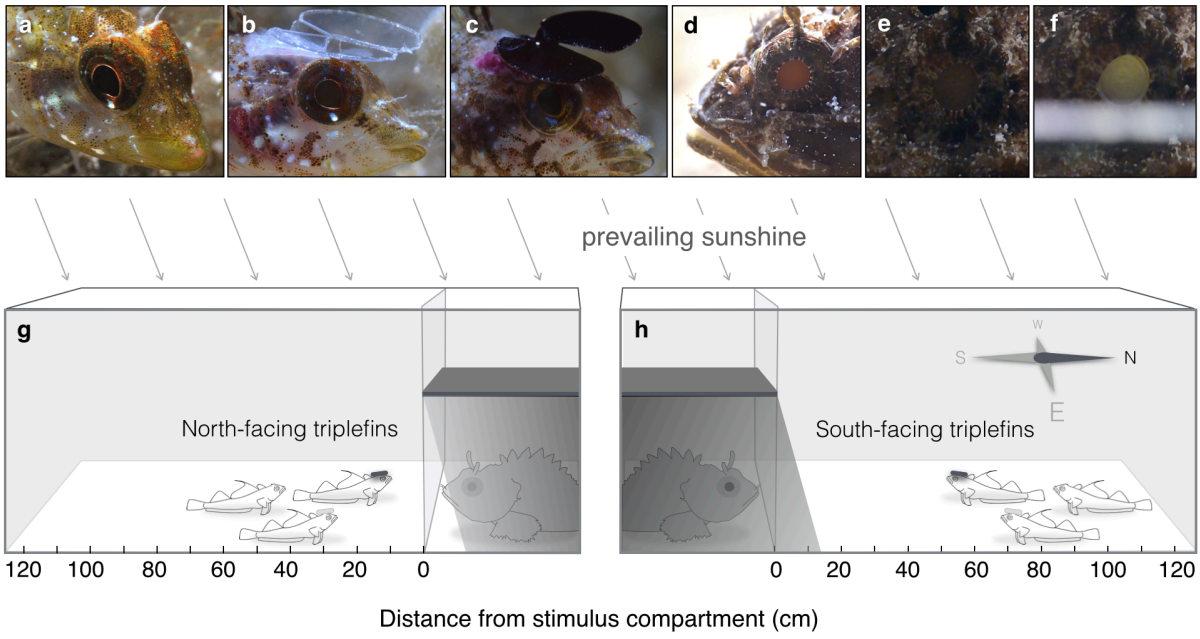

Fig. 1. Experimental manipulation and design. Triplefins (*Tripterygion delaisi*) were subjected to one of three treatments: **a**, Unhatted sham control, **b**, Clear-hatted control, and **c**, Shading hat. Whereas **a** and **b** can re-direct light using ocular sparks, visible as bright white dots on the lower iris, **c** cannot. **d**, Their cryptobenthic predator, a scorpionfish (*Scorpaena porcus*), shows retroreflective eyeshine[13] when illuminated coaxially, here by means of a narrow strip of white paper (compare **e** and **f**). **g**-**h**, Triplets of triplefins containing one fish from each treatment were visually exposed to a predator (deterrent) or a stone (attractant, not shown). In the field, we tested two opposite orientations relative to the sun (as shown), which was not necessary for the artificial illumination used under laboratory conditions (not shown). Distance from the stimulus was the response variable. Drawings not to scale, see methods for dimensions. Pictures by M.S. and N.K.M.

Retroreflective eyeshine is a widespread property of focusing eyes that possess a reflective inner layer behind the retina[11], such as a *tapetum lucidum* or a *stratum argenteum*. Retroreflective eyes make ideal detection targets because they return light to the source with a very narrow beamspread[12] that can only be induced and seen by an organism with a near-coaxial light source adjacent to the detecting pupil. Retroreflection is so efficient that even weak near-coaxial light can generate perceptible eyeshine in a retroreflective target (Fig. 1e). Although retroreflective eyeshine is best known from nocturnal animals, it also occurs in some diurnal species such as scorpionfish[13] (Fig. 1d-f).

Here, we experimentally tested whether redirection of light by irides helps triplefins detect a cryptic predatory scorpionfish. We suppressed ocular spark generation by gluing opaque mini-hats onto triplefins (Fig. 1c). Two control treatments permitted regular ocular spark formation: a clear-hatted (Fig. 1b) and an unhatted sham control (Fig. 1a). Triplefins were tested in triplets consisting of one individual of each treatment. Pilot experiments confirmed that typical behaviours such as fin flicks, push-ups, active movement across the substrate, and head and eye movements did not differ between shading and control treatments[14]. The experimental results presented here also indicated no difference in overall response and behaviour other than in predator detection.

Results

Response to a cryptic predator in a laboratory experiment

In a laboratory experiment, we visually exposed triplefins to a scorpionfish and a stone in an otherwise stone-free aquarium for two days, but with only one of the two stimuli visible on a given day. Given their preference for rocky substrates, the stone served as an attractor and positive control, whereas the scorpionfish was predicted to have a deterrent effect. We noted the distance to the visual stimulus five times per day. We found that all triplefin individuals were positioned farther from the predator than from the stone (Fig. 2). A comparison of the two controls (unhatted versus clear hatted sham treatment) (Fig. 2a) showed that the stimulus effect did not different between the two control hat treatments (Linear Mixed Effects Model LMEM: $R^2_{marg} = 0.30$, $R^2_{cond} = 0.31$, hat treatment $p = 0.66$, stimulus $p < 0.0001$, hat treatment x stimulus $p = 0.41$, stimulus order $p = 0.10$). For subsequent comparisons, controls were averaged per triplet, allowing the inclusion of triplets in which the clear-hatted individual had lost its hat prematurely. A comparison of averaged controls against the shading hat treatment (Fig. 2b) confirmed the overall effect of the stimulus (LMEM: $R^2_{marg} = 0.28$, $R^2_{cond} = 0.28$: hat treatment $p < 0.0001$, stimulus $p < 0.0001$, stimulus order $p = 0.04$), but now this effect also varied with hat treatment (hat treatment x stimulus $p = 0.016$). Relative to the controls, shaded individuals stayed significantly closer to the scorpionfish (LMEM for stimulus scorpionfish: $R^2_{marg} = 0.14$, $R^2_{cond} = 0.23$: hat treatment $p < 0.0001$, stimulus order $p = 0.31$) but not to the stone (LMEM for stimulus stone: $R^2_{marg} = 0.02$, $R^2_{cond} = 0.02$: hat treatment $p = 0.21$, stimulus order $p = 0.16$).

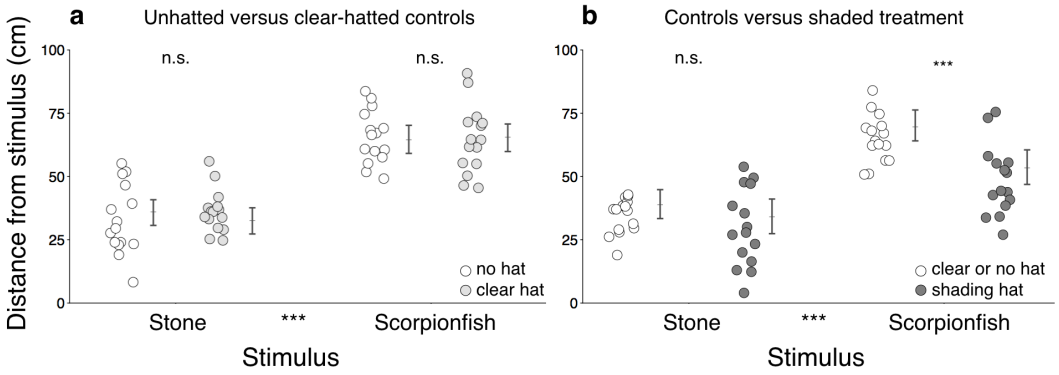

Fig. 2. Consequences of hatting in the laboratory: Distance from the stimulus as a function of stimulus type (stone or scorpionfish) and hat treatment. **a**, Fish in the two control treatments did not differ in how much they were attracted to the stone or deterred by the scorpionfish. **b**, Relative to the per-triplet averaged controls, shaded individuals stayed significantly closer to the scorpionfish. Symbols = average of 5 measurements per triplet; n = 15 triplets; error bars: model-predicted group means ± 95 % credible intervals; *** = $p < 0.001$, n.s. = $p > 0.05$ (see text and methods for details). Note that statistical comparisons were made between treatments *within* triplets, making group means and error bars poor predictors of statistical significance.

Response to a cryptic predator in a field experiment

In a field-replicate of this experiment, we placed 10 translucent tanks on the sea floor at 15 m depth (Fig. 1g-h). Anticipating a possible effect of orientation in relation to the sun, five tanks were oriented north, another five south (Fig. 1h) without *a priori* expectation. The distance to the stimulus was determined while SCUBA diving three times per day. In agreement with the laboratory experiment (Fig. 2), fish in the field also stayed closer to the stone than to the scorpionfish, regardless of the hatting treatment (Fig. 3). Likewise, the two control treatments kept similar distances within each combination of stimulus and orientation (Fig. 3a). However, south-facing controls responded clearly stronger to the scorpionfish relative to the stone than north-facing controls, resulting in a strong stimulus x orientation interaction (LMEM: $R^2_{marg} = 0.31$, $R^2_{cond} = 0.56$: hat treatment $p = 0.670$, stimulus $p < 0.0001$, hat treatment x stimulus $p = 0.48$, orientation $p = 0.37$, stimulus x orientation $p < 0.0001$, stimulus order $p = 0.004$).

Given this strong orientation effect, we performed the core analysis comparing the per-triplet averaged controls with the shading treatment separately for the two orientations. In north facing triplefins (Fig. 3b), the effect of the hatting treatment differed between the two stimuli (LMEM: $R^2_{marg} = 0.23$, $R^2_{cond} = 0.45$: hat treatment $p = 0.75$, stimulus $p < 0.0001$, stimulus order $p < 0.0001$, hat treatment x stimulus $p = 0.037$). Shaded individuals stayed significantly closer than control individuals when exposed to a scorpionfish (LMEM for scorpionfish: $R^2_{marg} = 0.03$, $R^2_{cond} = 0.61$: hat treatment $p = 0.009$, stimulus order $p = 0.544$) but kept similar distances when exposed to a stone (LMEM stone: $R^2_{marg} = 0.16$, $R^2_{cond} = 0.73$: hat treatment $p = 0.094$, stimulus order $p = 0.025$).

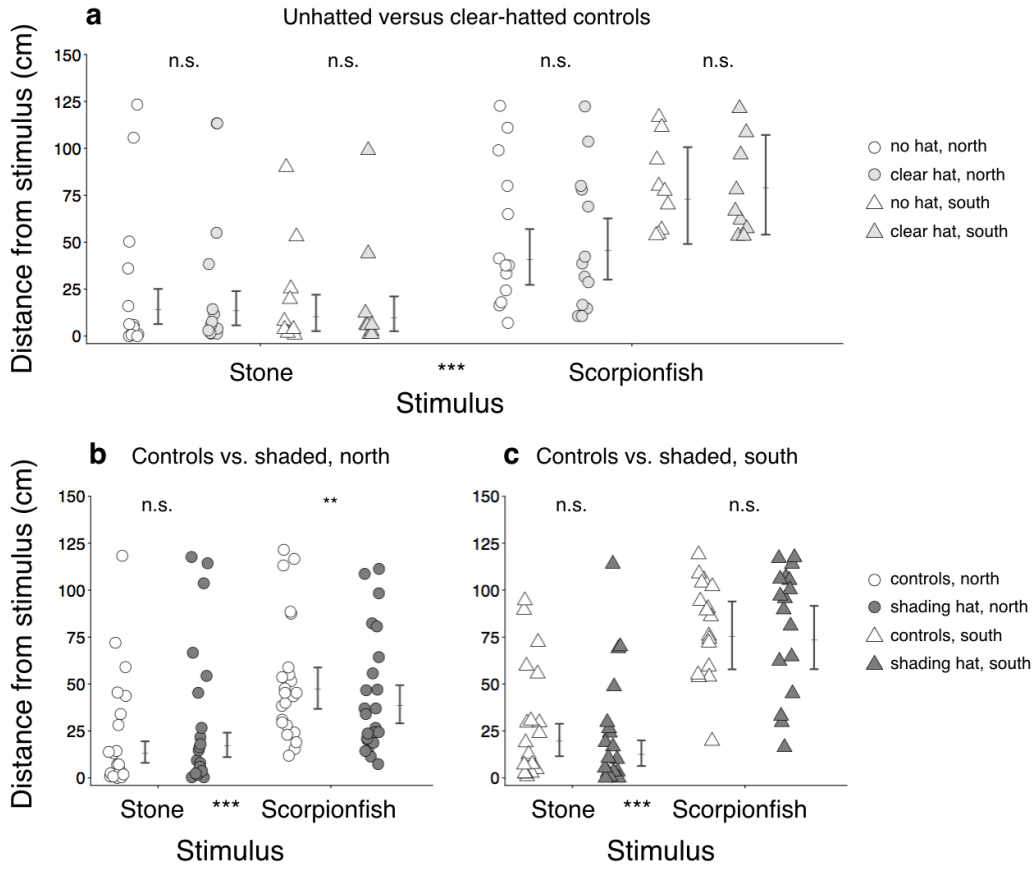

Fig. 3. Consequences of hatting in the field: Distance from stimulus as a function of stimulus type (stone or scorpionfish) and hat treatment. **a**, Controls did not differ in response, but south-facing controls responded stronger (n = 22 triplets). **b**, In north-facing triplefins, shaded fish stayed closer to a scorpionfish than the per-triplet averaged controls (n = 21 triplets). **c**, In south-facing triplefins, such effect was absent (n = 19 triplets). Symbols: average of 3 measurements per individual; error bars: model-predicted means ± 95 % credible intervals. *** = $p < 0.001$, ** = $p < 0.01$, n.s. = $p > 0.05$ (see text and methods for details). Note that statistical comparisons were made between treatments *within* triplets, making group means and error bars poor predictors of statistical significance.

In south facing triplefins (Fig. 3c), shaded individuals did not differ from controls in the distances they kept to either stimulus (LMEM: $R^2_{marg} = 0.39$, $R^2_{cond} = 0.58$, hat treatment $p = 0.119$, stimulus $p < 0.0001$, hat treatment x stimulus $p = 0.247$). When facing south, triplefins appear to have experienced light conditions that facilitated detection of a camouflaged scorpionfish from greater distances through regular vision, precluding the benefits that active photolocation offers over short distances. It is a reminder that active photolocation is not a mandatory requirement for detection. It supplements regular vision and may only offer an advantage under conditions where a scorpionfish is so well-camouflaged that regular vision fails to detect it leading to short approaching distances. This could explain the outcome in north-facing triplefins, where all treatments approached the scorpionfish more closely, and explain why the effect caused by the shading treatment is significant at short range (north-facing), but not at long range (south-facing).

Modelling visual detection of self-induced predator eyeshine by a triplefin

To validate our experimental results, we implemented visual models to compute the contrast change in the pupil of a scorpionfish perceived by an untreated triplefin when switching its ocular spark from *off* to *on*. Even when not illuminated by an ocular spark, the pupil of a scorpionfish is not black, but shows a certain luminance, which helps concealing the pupil[13]. This baseline pupil brightness will vary with the degree of shading and the substrate on which the scorpionfish sits. Here, we limit ourselves to parameter settings matching the light conditions of the field experiment and focus on modelling the effect of blue ocular sparks (Fig. 1a, b; see [3] for spark types). Relative to a white standard, blue ocular sparks have an average reflectance of 1.34 over the 400-700 nm range, with a maximum average of 2.15 at 472 nm, illustrating the effect of light focussing by the lens[3]. Further parameters included ambient light estimates in the field tanks, scorpionfish pupil size, baseline radiance (Fig. 1d) and reflective properties[13], and the triplefin visual system[15]. We used the receptor-noise model[16] for estimating chromatic contrasts and Michelson contrasts using cone-catch values for achromatic contrasts.

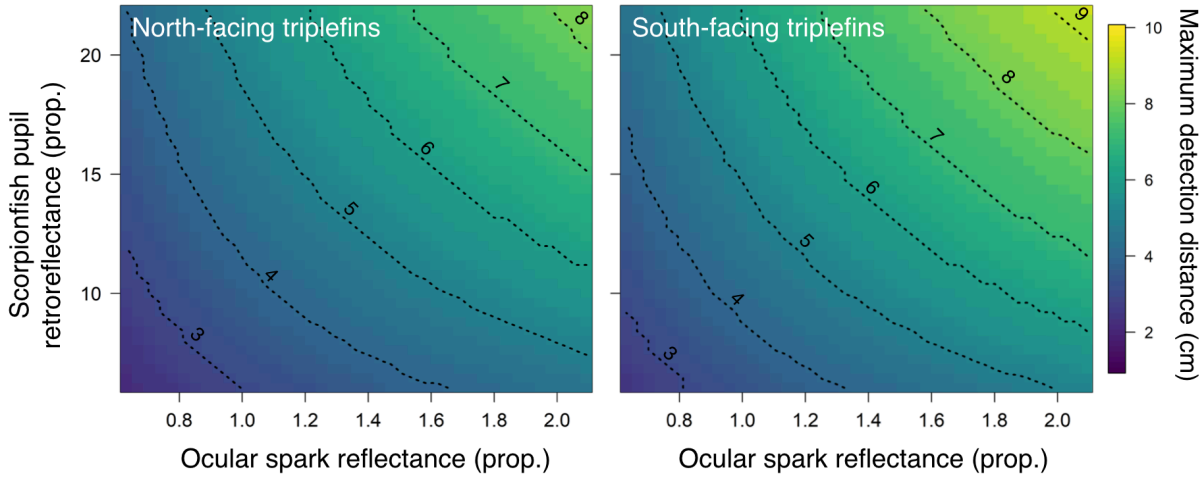

Fig. 4. Theoretical detection distance by a triplefin of a blue ocular spark reflected by a scorpionfish's eye. Visual modelling outputs show maximum detection distance (colour) of achromatic contrast differences in a scorpionfish's pupil as triggered by a triplefin's blue ocular spark. The outcome is shown as a function of ocular spark reflectance and scorpionfish pupil retroreflectance, separated by triplefin orientation (Fig. 1g-h). Values were obtained from calculating the Michelson contrast based on triplefins' cone-catches for each millimetre between 1 and 15 cm, and identifying the maximum distance at which the contrast was equal to or exceeded the achromatic contrast threshold of *T. delaisi* (0.8 % [17]). Both axes cover the range of measured values.

Ocular sparks did not generate chromatic contrast above discriminability threshold at any distance between the triplefin and scorpionfish but produced detectable achromatic contrasts across a broad range of conditions (Fig. 4). For north-facing triplefins, the reflection of the ocular spark from a scorpionfish's pupil would be detectable from ~5 cm

under average conditions. In situations where ocular spark radiance and scorpionfish eye retroreflectance exhibit greater values, the reflection of the ocular spark would be detectable from over 8 cm. The calculated detection distances increase slightly for triplefins facing south. Recognising a predator at these distances is likely to reduce the probability of capture by scorpionfish since they strike over short distances only[18-20]. For comparison, identical calculations for spark-generated contrast changes in a scorpionfish's iris rather than pupil showed no perceptible effect under any of the tested conditions. This confirms that subocular light emission is too weak to generate a contrast in another structure than a strong directional reflector such as a retroreflective eye. Note that the maximum detection distances predicted by the model are generally shorter than the distances observed by means of point observations in the two experiments. This discrepancy follows from the fact that the empirical data do not represent the distance of detection or closest approach. We expect free-moving triplefins to stay *outside* the area of detection. Hence, the observed distances are expected to be longer than the detection distances predicted by the model.

Discussion

Our results provide direct evidence for the diurnal active photolocation hypothesis by showing that small benthic fish can significantly increase the distance at which they detect pupil eyeshine in life-threatening predators by redirecting downwelling light via their irides. The properties described here for one triplefin and one scorpionfish species are not unique: mechanisms for light redirection are widespread and diverse across diurnal fish families[3,21], as are retroreflective eyes featured by cryptic predators[13]. Diurnal active photolocation could therefore be an important, yet previously neglected vision enhancement mechanism, and thus represent a significant force in the evolution of fish eyes.

Methods

Model species

Tripterygion delaisi is a small (4–5 cm) NE-Atlantic and Mediterranean micro-predatory triplefin species (Fam. Tripterygiidae) found on rocky substrates at 5 to 20 m depth (max 1 to 50 m). Aside from breeding males, it is highly cryptic and regularly produces blue and red ocular sparks[3]. *Scorpaena porcus* (Fam. Scorpaenidae) is a cryptobenthic sit-and-wait predator (12–20 cm) from coastal marine hard substrates and seagrass habitats across the NE-Atlantic and Mediterranean Sea[22]. Small benthic fish, such as triplefins, are often a component of its diet[23]. It possesses a reflective *stratum argenteum* and partially translucent retinal pigment epithelium that allows for the generation of daytime eyeshine, which is considered to be a form of pupil camouflage[13]. All experiments were conducted in

Calvi (Corsica, France) under the general permit of STARESO (Station de Recherches Sous Marines et Océanographiques).

Hatting technique to block ocular sparks

We prevented the formation of ocular sparks by fitting triplefins with plastic mini-hats from polyester filters excised using a laser cutter (RLS 100, AM Laserpoint Deutschland GmbH, Hamburg, Germany). A dark red filter with average transmission 1 % was used as the shading treatment (LEE #787 “Marius Red”, LEE Filters, UK). Clear filter hats (LEE #130, “Clear”) were used in the first control group, and no hat, but the same handling procedure, in the second control group. Hats were individually adjusted with clippers and folded into their final configuration with a triangular base for attachment and raised, forward-projecting wings to shade the eyes from downwelling light only. Hats formed an "umbrella" well above the eye, allowing full eye movement in all directions (Fig. 1b-c). They varied from 6 to 9 mm in diameter, matching individual head size. Given that *T. delaisi* possesses a fovea that is looking forward and downward when the eye is in a typical position, it seems unlikely that shading along may have resulted in poorer visual detection of a benthic predator in front of the fish relative to a triplefin without hat and without ocular spark. Animals in the clear-hatted and unhatted control groups regularly generated ocular sparks both in the laboratory and in the field.

Triplefins were collected using hand nets while SCUBA diving and brought to a stock aquarium in the laboratory. Individuals were anaesthetised (100 mg L^{-1} MS-222 in seawater, pH = 8.2) until all movements ceased except for breathing (3–4.5 min). Subsequently, the dorsal head surface was gently dried with paper tissue. Hats were glued to the triangular dorso-posterior head area just behind the eyes using surgical glue (Surgibond, Sutures Limited, UK). After allowing the glue to polymerise for 45 s, fish were moved into recovery containers with aerated seawater. Individuals regained consciousness and mobility within 5–10 min. This non-invasive hat fixation protocol minimised impacts on the fish's natural behaviour and health, as indicated by a 97.4 % survival rate. As a trade-off, however, hats detached within 0–4 days, which reduced the number of triplets that could be used for analysis (see Statistical analysis). All fish were treated and included in trials once and only returned to the field after completion of the experiment.

Laboratory experiment

Four tanks (L × W × D: 130 × 50 × 50 cm^3) were used for 20 experimental runs, each employing a new triplet of size-matched *T. delaisi*. In each tank, we placed a rock and a scorpionfish in two separate perforated containers (L × W × H: 24 × 14 × 16 cm^3) with a glass front. Both stimuli were simultaneously present in the tank, but only one was visible to the triplefins. The bottom of the aquarium was barren (avoided by the fish), except for a 10 cm strip of gravel placed along the long side of the tank, providing a sub-optimal substrate. Each tank was illuminated with a 150 W cold white LED floodlight (TIROLED Hallenleuchte,

150 W, 16000 Lumen) shielded with a LEE Filters #172 Lagoon Blue filter to simulate light at depth. The area of the tank where stimuli were displayed was shaded. All triplets were exposed to each stimulus for one full day. Since fish are moving regularly, we assessed the distance to the stimulus five times per day, at 0800, 1100, 1300, 1500 and 1800. Stimuli were presented in random order.

Field experiment

We replicated the previous experiment in the field using ten tanks of spectrally neutral Evotron Plexiglas (L × W × D: 150 × 25 × 50 cm^3) placed at 15 m depth on sandy patch in the seagrass meadow in front of STARESO. We used local silica sand mixed with gravel as substrate. Visual contact between tanks was excluded by surrounding each enclosure with 10 cm white side covers. As a response variable, we noted the distance of each individual from the stimulus compartment three times a day at 0900, 1200 and 1500 for two days following deployment in the early evening of the first day. Stimuli were always changed after the first observation day. Triplets were replaced every three days. In total, 75 triplets were tested.

Statistical analysis

Behavioural data were analysed using Linear Mixed Effects Models (LMEM) with the lme4 package[24] for R v3.3.2.[25]. For both experiments, we first compared the two control treatments (sham and clear hat) to verify that hatting a fish did not affect behaviour, and to confirm their ability to distinguish a cryptic predator from a stone. Because controls did not differ, we averaged their data per triplet for the final models and compared them to the shaded treatment. This allowed us to include triplets in which only the clear-hatted fish had lost its hat for the comparison with the shaded fish (such triplets were excluded from the comparison of the controls). This explains the variation in triplet numbers in the final analyses. Distance from the display compartment was used as the response variable in both models.

For the laboratory experiment, the initial fixed model component included the main predictors *stimulus* (stone *vs* scorpionfish), *hat treatment* (no hat *vs* clear hat, or averaged controls *vs* shaded) and their interaction. We further included the fixed covariates *daytime*, *stimulus order, cohort and tank ID.* The models for the replicated field experiment were identical, but also included the fixed factor *orientation* (north or south) and its interactions with the main factors. We also square-root-transformed the response variable *distance* to improve residual homogeneity. The transformation of the response variable did not cause any change in the effects of the interactions between covariates. Models to compare the response of controls *vs* shaded fish were calculated separately for north *vs* south orientation because fish responded differently to the scorpionfish depending on orientation (Fig. 3).

In all models, the initial random component contained triplet ID with random slopes over the hat treatment. This accounts for the repeated measurements of each triplet and captures variation arising from different hat-treatment responses among triplets[26]. Random slopes were uninformative and subsequently removed. We then performed backward model selection using the Akaike Information Criterion (AIC) to identify the best-fitting model with the smallest number of covariates[27]. We only report the reduced final models and provide proxies for their overall goodness-of-fit (marginal and conditional R^2) using pairwiseSEM[28]. The marginal R^2 expresses the proportion of variation explained by the model considering fixed factors only, whereas the conditional R^2 expresses the same including the random factors[29]. We used Wald *z*-tests to assess the significance of fixed effects. To explore significant interactions between stimulus and hat treatment, we implemented new models within the two levels of the stimulus treatment. Model assumptions were validated by plotting residuals versus fitted values and each covariate present in the full, non-reduced model[30].

Estimating scorpionfish pupil radiance with and without ocular spark

We assumed both triplefins and scorpionfish were looking orthogonally at one another to calculate the photon flux of the scorpionfish pupil reaching the triplefin, with and without the contribution of a blue ocular spark (SI 1). Using retinal quantum catch estimates, we calculated the chromatic contrast[16] between the scorpionfish pupil with and without ocular sparks. The achromatic contrast between the same two conditions was estimated by calculating the Michelson contrast for the quantum catches of the two-long-wavelength photoreceptors. For comparison, we also performed the same calculations using photon flux from the scorpionfish iris with and without the contribution of an ocular spark. We parameterized the equations using measurements of: (1) ambient light in the tanks at 15 m depth, (2) the range of ocular spark radiance under downwelling light conditions, (3) baseline scorpionfish pupil radiance in the experimental tanks, (4) sizes of triplefin pupil, ocular spark and scorpionfish pupil, and (5) scorpionfish pupil and iris reflectance[13].

Spectroradiometric measurements were obtained with a calibrated SpectraScan PR-740 (Photo Research, New York USA) encased in an underwater housing (BS Kinetics, Germany). This device measures spectral radiance (watts sr^{-1} m^{-2} nm^{-1}) of an area with defined solid angle. The downwelling light was estimated by measuring the radiance of a polytetrafluoroethylene (PTFE) diffuse white reflectance standard (Berghof Fluoroplastic Technology GmbH, Germany) positioned parallel to the water surface from a 45° angle. Radiance values were transformed into photon radiance (photons s^{-1} sr^{-1} m^{-2} nm^{-1}).

We determined the relationship between the radiance of the ocular spark and that of a white PTFE standard exposed to downwelling light in live triplefins. Fish mildly sedated with clove oil (n = 10) were placed in an aquarium illuminated with a Leica EL 6000 source and a liquid light guide suspended ~20 cm above the tank. Spark radiance was normalised by

comparing it to a white standard at 45° from normal positioned at the same location as the fish. For each fish, three measurements were obtained from each eye. The highest within-fish value relative to the standard was used for the model. The sizes of the triplefin pupil (*n* = 35), the ocular spark (*n* = 10), and the scorpionfish pupil (*n* = 20) were measured in ImageJ[31] using scaled images. Natural baseline pupil radiance of three different scorpionfish was measured orthogonally to the pupil from the perspective of the triplefins during the field experimental trials using a Photo Research PR-740 spectroradiometer.

Solid angles of the ocular spark as perceived from the perspective of the scorpionfish, and the pupil of the scorpionfish as perceived by the triplefin, were estimated through Monte Carlo simulations using SACALC3 v1.4[32]. Source and detector were both approximated as circular disks with the source radiating equally in all directions of a hemisphere (i.e. 2π steradians).

Visual models and maximum detection distance

The receptor-noise limited model for calculation of chromatic contrast was informed using triplefin ocular media transmission values, photoreceptor sensitivity curves[15,33], and the relative photoreceptor density of single to double cone of 1:4:4 as found in the triplefin fovea[34]. We used a Weber fraction (ω) value of 0.05 as in previous studies[35,36]. Chromatic contrasts are measured as just-noticeable differences (JNDs), where values >1 are considered to be larger than the minimum discernible difference between two objects. We calculated the Michelson achromatic contrast as

$$C = \frac{(Q_1 - Q_2)}{(Q_1 + Q_2)}$$

where Q_1 and Q_2 are the quantum catches of the two members of the double cones which are associated with the achromatic channel, under photon $flux_1$ and photon $flux_2$. $Flux_1$ is the sum of the photon flux into a triplefin's eye caused by the baseline radiance of a scorpionfish pupil and the photon flux caused by the retroreflection of an ocular spark in the scorpionfish pupil (sum of equations (2) and (6) below). $Flux_2$ is calculated from the baseline radiance of a scorpionfish pupil only (no ocular spark reflection, equation (2) below). We determined the maximum discernible distance of the ocular spark radiance reflected through a scorpionfish pupil by calculating the chromatic and achromatic contrast at each millimetre, between 1 and 15 cm, and extracting the first value at which the contrast was equal to or exceeded 1.0 JND for chromatic contrasts and 0.008 for Michelson contrasts as measured in *T. delaisi*[17] and other fish species[37]. All visual models were performed using the R package pavo[38].

Table 1. Symbols used in the equations to calculate the photon flux of the scorpionfish pupil reaching the triplefin, with and without the contribution of an ocular spark.

Symbol	*Definitions and units*
L	Photon radiance (photons s^{-1} sr^{-1} m^{-2})
S	Blue ocular spark reflectance (proportion in relation to PTFE white standard)
d	Distance between triplefin and scorpionfish (m)
r_t	Radius of triplefin pupil (m)
R	Reflectance of coaxially illuminated scorpionfish pupil (prop. in relation to PTFE white standard)
κ	Diffuse attenuation coefficient (m^{-1})
Φ	Photon flux (photons s^{-1})
Ω	Solid angle (sr)

Visual model details

Triplefin – scorpionfish interaction

The starting conditions assume that both fish look at each other at normal incidence, i.e. the full area of the pupil of the triplefin is visible to the scorpionfish and vice versa. Solid angles are computed as explained below, assuming the ocular spark is positioned at the edge of the iris (displacement = 1.09 mm) in the plane of the triplefin pupil.

Photon flux without ocular spark

The photon radiance of the scorpionfish pupil reaching the triplefin (L_d) is a function of the measured scorpionfish pupil photon radiance (L_0) attenuated by the aquatic medium over distance *d* such that

$$L_d = L_0 \times e^{-\kappa d} \quad (1)$$

The photon flux reaching the retina of the triplefin without the ocular spark (Φ_{ns}) (Fig. 5) is the proportion of attenuated photon radiance reaching the triplefin's pupil (L_d) multiplied by the solid angle of the scorpionfish pupil (Ω_{sp}) and the area of the triplefin pupil (πr_t^2):

$$\Phi_{ns} = L_d \times \Omega_{sp} \times \pi r_t^2 \quad (2)$$

This value was used to calculate the quantum catches Q_1 and Q_2 mentioned earlier.

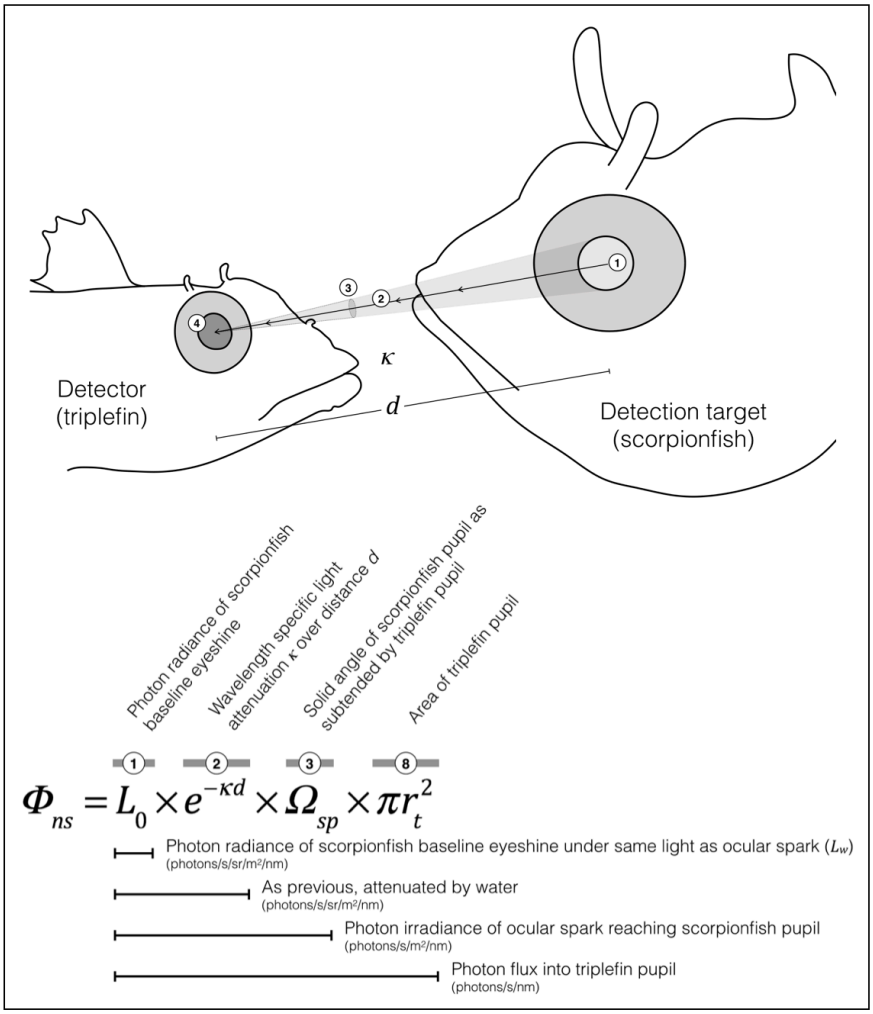

Fig. 5: Visual representation of how the photon flux $\boldsymbol{\Phi}_{ns}$ originating from baseline scorpionfish eyeshine entering a triplefin's pupil is calculated. This case excludes the effect of an ocular spark, which is shown in Fig. 6.

Photon flux with ocular spark

The photon radiance of the ocular spark reaching the scorpionfish (L_{os}) is a function of the radiance of a PTFE white standard parallel to the water surface (L_w), the focussing power of the lens, and the reflective properties of the iridal chromatophores on which the light is focused. For now, the focussing power and reflective properties have only been measured together as blue ocular spark reflectance (S) relative to L_w:

$$L_{os} = L_w \times S \times e^{-\kappa d} \quad (3)$$

The radiance of the scorpionfish pupil (L_{sp}) defined as the proportion of the attenuated ocular spark photon radiance that reaches the scorpionfish pupil and is re-emitted towards the triplefin is estimated by multiplying the photon radiance of the ocular spark reaching

the scorpionfish (L_{os}) with the solid angle of the ocular spark as seen by the scorpionfish (Ω_{os}) and the retroreflectance of the scorpionfish pupil with illumination co-axial to the receiver (R). Because the properties of the retroreflective eye are measured in relation to a diffuse white standard, the photon exitance from the scorpionfish pupil is converted to photon radiance by dividing by π steradians:

$$L_{sp} = L_{os} \times \Omega_{os} \times R \times \pi^{-1} \quad (4)$$

The scorpionfish pupil radiance (L_{sp}) travelling towards the triplefin pupil is further attenuated, and the photon flux reaching the triplefin's retina (Φ_{os}) is obtained by multiplying the attenuated radiance by the solid angle of the scorpionfish pupil, and the area of the triplefin pupil:

$$\Phi_{os} = L_{sp} \times e^{-\kappa d} \times \Omega_{sp} \times \pi r_t^2 \quad (5)$$

The photon flux generated by the ocular spark, which reaches the triplefin retina after being reflected by the scorpionfish pupil is therefore approximated by (see also Fig. 6):

$$\Phi_{os} = L_w \times S \times e^{-\kappa d} \times \Omega_{os} \times R \times \pi^{-1} \times e^{-\kappa d} \times \Omega_{sp} \times \pi r_t^2 \quad (6)$$

The total photon flux reaching the retina of the triplefin with the ocular spark is then the sum of equations (2) and (6) (Figs. 5 and 6 combined). This sum was used to calculate the quantum catches Q_1 and Q_2 from a scorpionfish eye illuminated by an ocular spark, as mentioned earlier.

The mean solid angle of the scorpionfish pupil from the perspective of the triplefin eye (Ω_{sp}), and the solid angle of the ocular spark from the perspective of the scorpionfish eye (Ω_{os}) at distance *d* was estimated by Monte Carlo simulations[32].

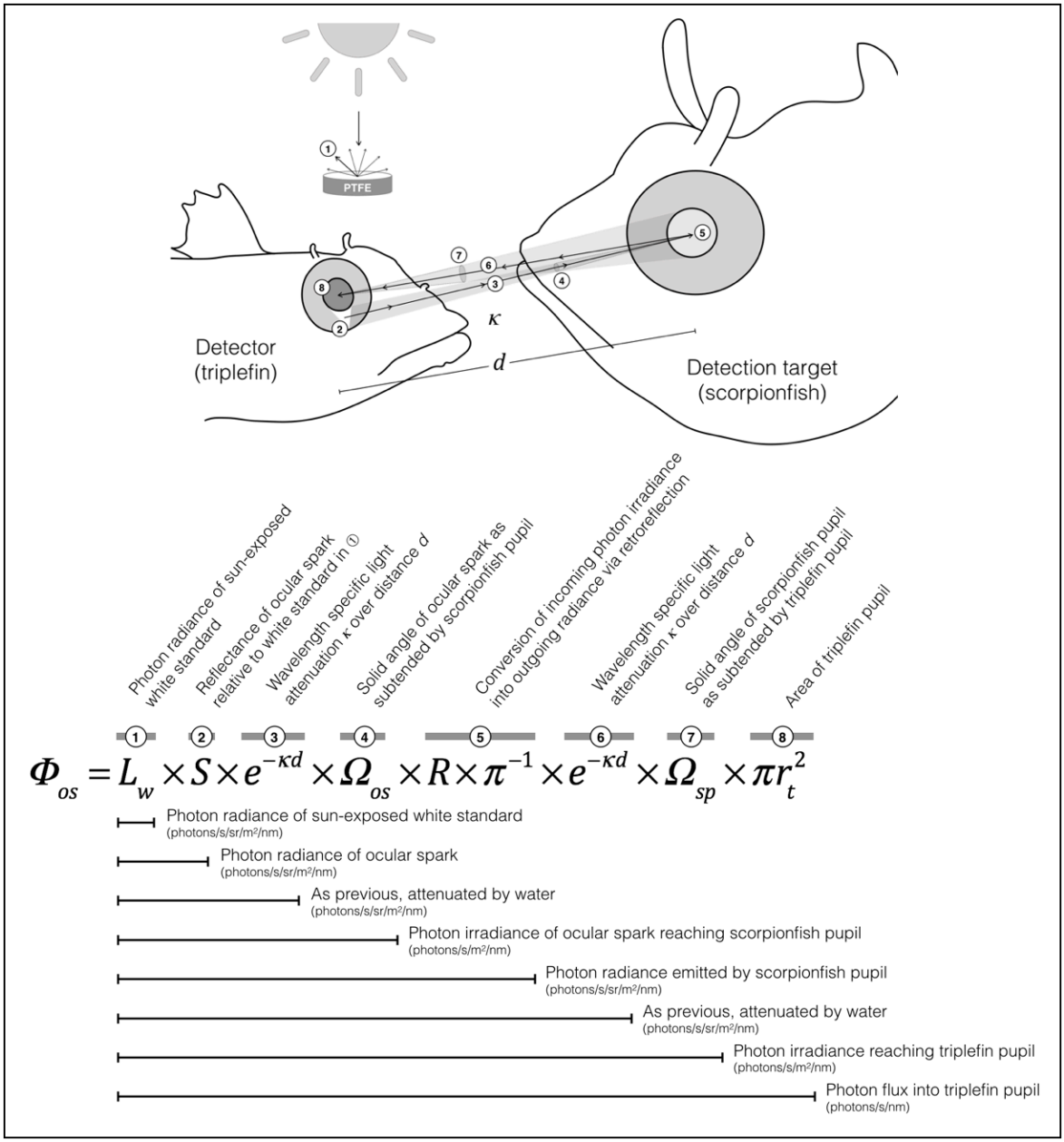

Fig. 6: Visual representation of how much of the photon flux Φ_{ns} generated by a triplefin's ocular spark is reflected as scorpionfish eyeshine and ultimately reaches a triplefin's pupil. This effect needs to be added on top of baseline scorpionfish eyeshine (explained in Fig. 5), to obtain the total photon flux from a scorpionfish eye reaching the eye of a triplefin with its ocular spark on.

Data availability

Materials & correspondence: Raw data and the R-scripts of the experiments and the visual modelling are available on request from N.K.M. (nico.michiels@uni-tuebingen.de), M.S. (matteo.santon@uni-tuebingen.de) and P.P.B. (pbitton@mun.ca). They will be made available in dryad upon acceptance (**link to be added**).

References

1 Howland, H. C., Murphy, C. J. & McCosker, J. E. Detection of eyeshine by flashlight fishes of the family Anomalopidae. *Vision Res* **32**, 765-769, doi:10.1016/0042-6989(92)90191-k (1992).

2 Hellinger, J. *et al*. The Flashlight Fish *Anomalops katoptron* Uses Bioluminescent Light to Detect Prey in the Dark. *PLoS ONE* **12**, e0170489, doi:10.1371/journal.pone.0170489 (2017).

3 Michiels, N. K. *et al*. Controlled iris radiance in a diurnal fish looking at prey. *R Soc open sci* **5**, 170838, doi:10.1098/rsos.170838 (2018).

4 Lythgoe, J. N. *The Ecology of Vision*. (Clarendon Press, 1979).

5 Sutton, T. T. Trophic ecology of the deep-sea fish *Malacosteus niger* (Pisces: Stomiidae): An enigmatic feeding ecology to facilitate a unique visual system? *Deep-Sea Res Part I Oceanogr Res Pap* **52**, 2065-2076, doi:10.1016/j.dsr.2005.06.011 (2005).

6 Douglas, R. H., Mullineaux, C. W. & Partridge, J. C. Long-wave sensitivity in deep-sea stomiid dragonfish with far-red bioluminescence: evidence for a dietary origin of the chlorophyll-derived retinal photosensitizer of *Malacosteus niger*. *Philos Trans R Soc Lond B Biol Sci* **355**, 1269-1272, doi:10.1098/rstb.2000.0681 (2000).

7 Douglas, R. H. *et al*. Enhanced retinal longwave sensitivity using a chlorophyll-derived photosensitiser in *Malacosteus niger*, a deep-sea dragon fish with far red bioluminescence. *Vision Res* **39**, 2817-2832, doi:10.1016/S0042-6989(98)00332-0 (1999).

8 Kenaley, C. P., Devaney, S. C. & Fjeran, T. T. The complex evolutionary history of seeing red: molecular phylogeny and the evolution of an adaptive visual system in deep-sea dragonfishes (Stomiiformes: Stomiidae). *Evolution* **68**, 996-1013, doi:10.1111/evo.12322 (2014).

9 Sutton, T. T. & Hopkins, T. L. Trophic ecology of the stomiid (Pisces: Stomiidae) fish assemblage of the eastern Gulf of Mexico: Strategies, selectivity and impact of a top mesopelagic predator group. *Mar Biol* **127**, 179-192, doi:10.1007/bf00942102 (1996).

10 Jack, C. B. *Detecting the Detector: A Widespread Animal Sense?*, <http://vixra.org/abs/1411.0226> (2014).

11 Fritsch, R., Ullmann, J. F. P., Bitton, P. P., Collin, S. P. & Michiels, N. K. Optic-nerve-transmitted eyeshine, a new type of light emission from fish eyes. *Front Zool* **14**, 14, doi:10.1186/s12983-017-0198-9 (2017).

12 Von Helmholtz, H. *Handbuch der physiologischen Optik*. Vol. 9 (Voss, 1867).

13 Santon, M., Bitton, P. P., Harant, U. K. & Michiels, N. K. Daytime eyeshine contributes to pupil camouflage in a cryptobenthic marine fish. *Sci Rep* **8**, 7368, doi:10.1038/s41598-018-25599-y (2018).

14 Dehm, J. *Does wearing a hat change the demeanour of a fish? A behavioural study of the manipulation of active photolocation in the benthic fish Tripterygion delaisi* MSc thesis, University of Kiel, (2015).

15 Bitton, P.-P. *et al*. Red fluorescence of the triplefin *Tripterygion delaisi* is increasingly visible against background light with increasing depth. *R Soc open sci* **4**, 161009, doi:10.1098/rsos.161009 (2017).

16 Vorobyev, M. & Osorio, D. Receptor noise as a determinant of colour thresholds. *Proc R Soc B Biol Sci* **265**, 351-358, doi:DOI 10.1098/rspb.1998.0302 (1998).

17 Santon, M., Münch, T. A. & Michiels, N. K. The contrast sensitivity function of a small cryptobenthic marine fish. *Journal of Vision* (*submitted*).

18 Montgomery, J. C. & Hamilton, A. R. Sensory contributions to nocturnal prey capture in the dwarf scorpion fish (*Scorpaena papillosus*). *Mar. Fresh. Behav. Physiol.* **30**, 209-223, doi:Doi 10.1080/10236249709379026 (1997).

19 La Mesa, M., Scarcella, G., Grati, F. & Fabi, G. Age and growth of the black scorpionfish, *Scorpaena porcus* (Pisces: Scorpaenidae) from artificial structures and natural reefs in the Adriatic Sea. *Sci Mar* **74**, 677-685 (2010).

20 Harmelin-Vivien, M., Kaim-Malka, R., Ledoyer, M. & Jacob-Abraham, S. Food partitioning among scorpaenid fishes in Mediterranean seagrass beds. *J Fish Biol* **34**, 715-734 (1989).

21 Anthes, N., Theobald, J., Gerlach, T., Meadows, M. G. & Michiels, N. K. Diversity and ecological correlates of red fluorescence in marine fishes. *Front Ecol Evol* **4**, doi:10.3389/fevo.2016.00126 (2016).

22 Louisy, P. *Europe and Mediterranean marine fish identification guide*. (Ulmer, 2015).

23 Compaire, J. C., Casademont, P., Cabrera, R., Gómez-Cama, C. & Soriguer, M. C. Feeding of *Scorpaena porcus* (Scorpaenidae) in intertidal rock pools in the Gulf of Cadiz (NE Atlantic). *J Mar Biol Assoc U K*, 1-9 (2017).

24 Bates, D., Mächler, M., Bolker, B. M. & Walker, S. Fitting linear mixed-effects models using lme4. *J Stat Softw* **67**, 1-51 (2014).

25 R-Core-Team. *R: A language and environment for statistical computing*. (R Foundation for Statistical Computing, vienna, Austria, 2013).

26 Schielzeth, H. & Forstmeier, W. Conclusions beyond support: overconfident estimates in mixed models. *Behav Ecol* **20**, 416-420, doi:10.1093/beheco/arn145 (2009).

27 Zuur, A. F., Ieno, E. N., Walker, N. J., Saveliev, A. A. & Smith, G. M. *Mixed Effects Models and Extensions in Ecology with R*. (Springer, New York, 2009).

28 Lefcheck, J. S. & Freckleton, R. piecewiseSEM: Piecewise structural equation modelling inr for ecology, evolution, and systematics. *Methods Ecol Evol* **7**, 573-579, doi:10.1111/2041-210x.12512 (2016).

29 Nakagawa, S. & Schielzeth, H. Repeatability for Gaussian and non-Gaussian data: a practical guide for biologists. *Biol Rev* **85**, 935-956, doi:10.1111/j.1469-185X.2010.00141.x (2010).

30 Zuur, A. F., Ieno, E. N. & Freckleton, R. A protocol for conducting and presenting results of regression-type analyses. *Methods Ecol Evol* **7**, 636-645, doi:10.1111/2041-210x.12577 (2016).

31 Abràmoff, M. D., Magalhães, P. J. & Ram, S. J. Image processing with ImageJ. *Biophotonics Int* **11**, 36-42 (2004).

32 Whitcher, R. A Monte Carlo method to calculate the average solid angle subtended by a right cylinder to a source that is circular or rectangular, plane or thick, at any position and orientation. *Radiat Prot Dosim* **118**, 459-474, doi:10.1093/rpd/nci381 (2006).

33 Govardovskii, V. I., Fyhrquist, N., Reuter, T., Kuzmin, D. G. & Donner, K. In search of the visual pigment template. *Visual Neurosci* **17**, 509-528, doi:10.1017/s0952523800174036 (2000).

34 Fritsch, R., Collin, S. P. & Michiels, N. K. Anatomical analysis of the retinal specializations to a crypto-benthic, micro-predatory lifestyle in the mediterranean triplefin blenny *Tripterygion delaisi*. *Front Neuroanat* **11**, 122, doi:10.3389/fnana.2017.00122 (2017).

35 Wilkins, L., Marshall, N. J., Johnsen, S. & Osorio, D. Modelling colour constancy in fish: implications for vision and signalling in water. *J Exp Biol* **219**, 1884-1892, doi:10.1242/jeb.139147 (2016).

36 Matz, M. V., Marshall, N. J. & Vorobyev, M. Are corals colorful? *Photochem Photobiol* **82**, 345-350, doi:10.1562/2005-08-18-RA-653 (2006).

37 Douglas, R. & Djamgoz, M. *The visual system of fish*. (Springer Science & Business Media, 2012).

38 Maia, R., Eliason, C. M., Bitton, P. P., Doucet, S. M. & Shawkey, M. D. pavo: an R package for the analysis, visualization and organization of spectral data. *Methods Ecol Evol* **4**, 906-913, doi:10.1111/2041-210x.12069 (2013).

Acknowledgments: We are indebted to the attendants of a workshop in November 2014 in Tübingen with Connor M. Champ, João Coimbra, Colin B. Jack, Sönke Johnsen, Almut Kelber, Melissa G. Meadows, Daniel Osorio, Shelby Temple and Annette Werner. Thanks to Martin J. How for useful suggestions on an earlier draft. Jonas Dornbach, Thomas Griessler, Katharina Hiemer, Michael Karcz, Valentina Richter, Peter Tung, Sabine Urban, Laura Warmuth and Florian Wehrberger supported data collection in the field. Gregor Schulte provided creative and technical support. Thanks to Pierre Lejeune, director of STARESO and his staff for providing excellent working conditions. N.K.M. was supported by Koselleck Grant Mi 482/13-1 from the Deutsche Forschungsgemeinschaft and Experiment! grant Az. 89148 and Az. 91816 from the Volkswagen Foundation. P-P.B. was funded by a Postdoctoral Fellowship from the Natural Sciences and Engineering Research Council of Canada.

Author contributions: N.K.M., R.F., M.S., P-P.B. and U.K.H. conceived the study. R.F. developed the hatting technique. N.K.M., J.D., M.S., U.K.H., R.F. and P-P.B. conceptualised the experiments. J.D. collected the laboratory data. M.S. and U.K.H. collected the field data, with assistance from the whole crew. M.S. and N.A. analysed the experimental data. P-P.B. developed and ran the visual model with support from M.S. using spectroradiometric data collected by M.S. and U.K.H. The manuscript was written by N.K.M., M.S., P.-P.B., R.F. and J.D. All authors edited and approved the manuscript.

Competing interests: The authors declare no competing interests.

Materials & correspondence: Raw data and the R-scripts of the experiments and the visual modelling are available on request from N.K.M. (nico.michiels@uni-tuebingen.de), M.S. (matteo.santon@uni-tuebingen.de) and P.P.B. (pbitton@mun.ca).